C2012-0001534

NACE INTERNATIONAL CORROSION 2012 CONFERENCE & EXPO

Top-of-the-Line Corrosion in The Presence of Hydrocarbon Co-Condensation in Flowing Condition

Thunyaluk Pojtanabuntoeng, Marc Singer, Srdjan Nesic[(1)]
Institute for Corrosion and Multiphase Technology
Ohio University
342 West State Street
Athens, OH 45701

ABSTRACT

During the transportation of wet gas, temperature gradient between the internals of the pipeline and the outside environment leads to the condensation of water vapor. Freshly condensed water is very corrosive and can lead to the so-called Top-of-the-Line Corrosion (TLC). However, a certain fraction of hydrocarbons will co-condense along with the water vapor resulting in two immiscible liquids at the pipe wall with a different wettability and different corrosivity. To elucidate the role of co-condensation, corrosion tests in the absence and presence of hydrocarbon were conducted.

In the experiments, hot vapors of water and n-heptane saturated with CO_2 were generated and transported through a one-inch internal diameter condenser tube, with 2 carbon steel samples located at the inlet and outlet of the tube. Condensation took place on the inner surface of the tube and was related to the TLC. Corrosion rate was evaluated by the weight loss method. In the absence of co-condensation, corrosion rates increased with water condensation rates. In the presence of n-heptane co-condensation, water condensation rates had less influence on the corrosion rates. Iron carbonate ($FeCO_3$) was observed only in the co-condensation scenario, suggesting the change of the chemistry of condensed water.

KEY WORDS: top of the line corrosion, co-condensation, CO_2 corrosion

[(1)] Corresponding author, E-mail address: nesic@ohio.edu (S. Nesic).

INTRODUCTION

In a wet gas transportation pipeline, Top-of-the-Line-Corrosion (TLC) is a serious concern due to the limited options for corrosion mitigation. Water condensation is the root cause of the problem. The gas is saturated with water vapor which will condense as temperature drops along the pipeline. Freshly condensed water is corrosive as it is saturated with CO_2, H_2S, acetic acid, etc. Extensive research has been conducted to better understand the TLC phenomena relating to these species.[1-3] However, until recently, no research has been conducted that involves the co-condensation of water and hydrocarbons. Since hydrocarbons are not corrosive, they are expected to provide a degree of protection to the pipelines when they co-condense on the carbon steel surface.

When water and hydrocarbon condense together, the condensate is made up of two immiscible liquids which have different wettabilities with respect to carbon steel. In work preceding the study reported herein, steel wettability phenomena relating to water and n-heptane were reported.[4] There, the condensation processes were visually observed and recorded. These results showed that carbon steel is hydrophilic, i.e. water is attracted more strongly than n-heptane to the steel surface. However, when both liquids co-condense, n-heptane seemed to segregate the water droplets and prevent their coalescence. This observation was in agreement with previous findings reported by other researchers.[5-7] For example, Akers reported that n-heptane and water condensed with a “Film-Drop” segregation pattern, in which water droplets are surrounded with n-heptane.[5] However, those studies focused on heat transfer rather than corrosion.

The influence of hydrocarbons on CO_2 corrosion has been extensively studied in bottom of the line applications, such as the inhibitive properties of different crude oils,[8-9] or relating to the hydrodynamic modeling of water entrainment.[10] It was found that light condensate did not provide much corrosion protection to the mild steel pipeline.[11] However, no studies of this kind were related to TLC scenarios.

In our previous studies, experiments were conducted in a stagnant condition, while water and n-heptane co-condensed.[4] The results showed that in the presence of n-heptane, there were distinctive corroded and non-corroded surface regions. Thus, the uniform corrosion rate was decreased. However, the thickness loss of metal was still comparable in the two cases. In that study, the condensation rate of both water and n-heptane was low, due to limitations with the experimental setup (low heat transfer rate in the stagnant vapor phase). A modification was made in the present study to achieve higher condensation rates, and mimic the TLC in the presence of n-heptane in a flowing condition.

EXPERIMENTAL

Apparatus and procedure

Top of the line corrosion was simulated in a flow tube design as shown in Figure 1. The use of n-heptane, as a representative hydrocarbon, presented certain experimental limitations due to safety concerns. Therefore, conditions were kept at atmospheric pressure and temperatures below 80^{o}C. A conventional glass condenser with a cooling water jacket was adapted to hold a

1 inch OD Teflon™ [1] tube which served as a sample holder. Carbon steel samples were flush mounted in the upper half of the tube at both ends (Figure 2). Temperature probes were positioned immediately below the carbon steel samples at the inlet and outlet of the condenser. Thus, the vapor temperature was constantly monitored throughout the test.

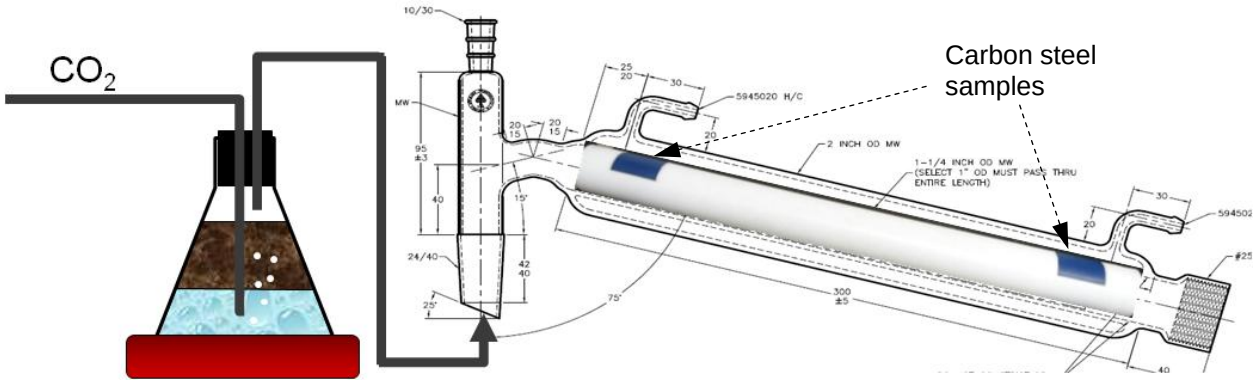

Figure 1: Schematic of the experimental setup for TLC study under flowing conditions.

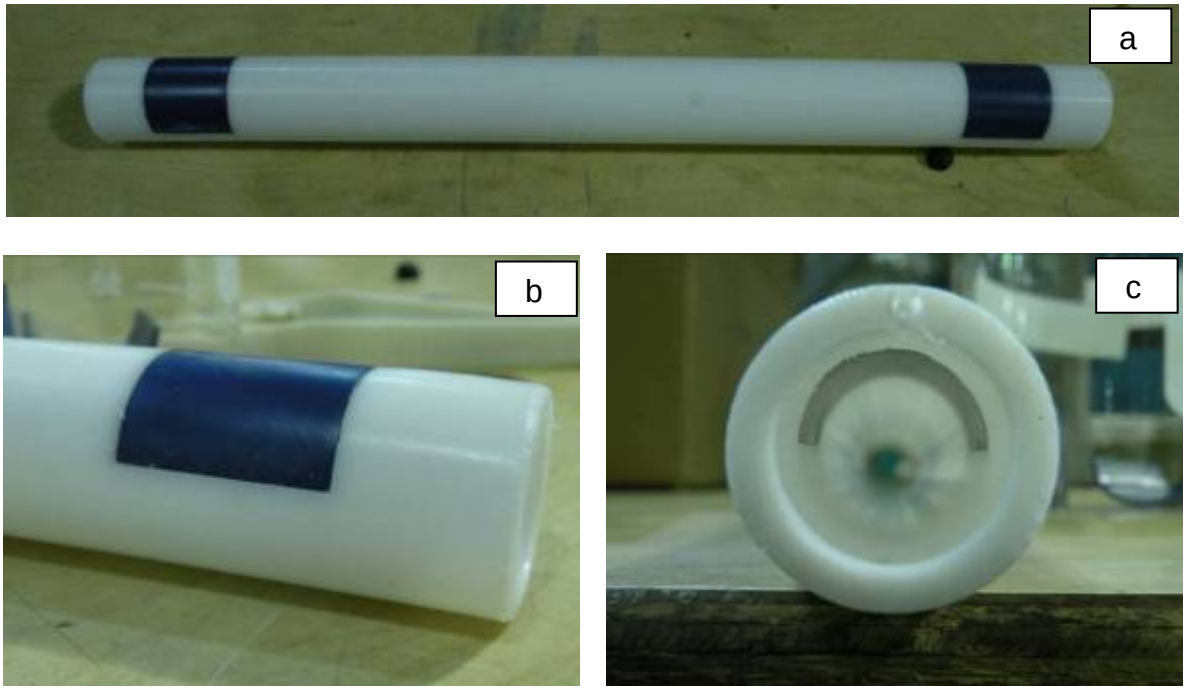

Figure 2: Images of the flow tube assembly with carbon steel samples: a) top view, b) side view, and c) cross section view

Water vapor saturated with CO_2 was generated in a separate Erlenmeyer flask. The CO_2, which served as a corrosive gas as well as the carrier gas, was bubbled at a constant rate throughout the test. Condensation rates were varied by adjusting the cooling water flow rate. The condensed liquids were collected and used to calculate the condensation rate. Since the vapor temperature decreased along the condenser, the condensation rate at the upstream

(1) Trade name.

carbon steel sample was higher than at the downstream one. Experiments lasted for 1 and 3 days. At the end of the experiment, the samples were removed, rapidly dehydrated and the Clarke solution [(2)] was used to remove any corrosion products from the surface.[12] The corrosion rate was obtained from weight loss. Scanning electron microscopy (SEM) and energy dispersive spectroscopy (EDX) were employed for surface analysis.

There were two series of experiments: (i) pure water condensation and (ii) co-condensation. Tables 1 and 2 describe the respective test conditions. Table 3 shows the chemical composition of the carbon steel sample.

Table 1
Test matrix for corrosion in pure water condensation

Parameters	Conditions
Steel type	X65
Vapor temperature (T_g), ^oC	18-65
Water condensation rate (WCR), mL/m^2/s	0.001-1
Total pressure, bar	1
Partial pressure of CO_2, bar	0.75-0.98
Test duration (days)	1, 3

Table 2
Test matrix for corrosion in co-condensation

Parameters	Conditions
Steel type	X65
Vapor temperature (T_g), ^oC	18-50
Hydrocarbon	n-heptane
Water condensation rate (WCR), mL/m^2/s	0.001-0.25
n-heptane condensation rate (HCCR) , mL/m^2/s	0.001-1.3
Total pressure, bar	1
Partial pressure of CO_2, bar	0.69-0.97
Test duration (days)	1, 3

Table 3
Compositional analysis of X65 carbon steel (the balance is Fe**)**

Element	Al	As	B	C	Ca	Co	Cr	Cu	Mn	Mo	Nb
%Wt.	0.032	0.008	0.001	0.13	0.002	0.007	0.14	0.131	1.16	0.16	0.017
Element	Ni	P	Pb	S	Sb	Si	Sn	Ta	Ti	V	Zr
%Wt.	0.36	0.009	<0.001	0.009	0.009	0.26	0.007	<0.001	<0.001	0.047	<0.001

(2) Trade name.

RESULTS AND DISCUSSION

Condensation rates

Since the experimental design allowed only the integrated condensation rate to be measured, one cannot directly determine the condensation rate at a specific location where the carbon steel samples were. A straight pipe heat transfer correlation[13] was employed to determine the temperature drop along the condenser. To do this, the length of the condenser was divided into 5 equal length sections. The calculated temperatures along the condenser length are plotted in Figure 3 and fit well with the gas temperature measurements at the inlet ($T_{gas,inlet}$) and outlet ($T_{gas,outlet}$). Subsequently, the condensation rate was calculated based on the temperature difference between the calculated vapor temperature and the cooling water temperature (T_{cw}) as shown in Figure 4. Predicted condensation rates, integrated over the length of the condenser, are plotted against the actual measurements in the parity plot shown in Figure 5. The good overall agreement indicates that the water condensation rates (WCR) on upstream and downstream samples are properly calculated. Hence, the condensation rates reported below refer to the calculated values at the upstream and downstream carbon steel samples.

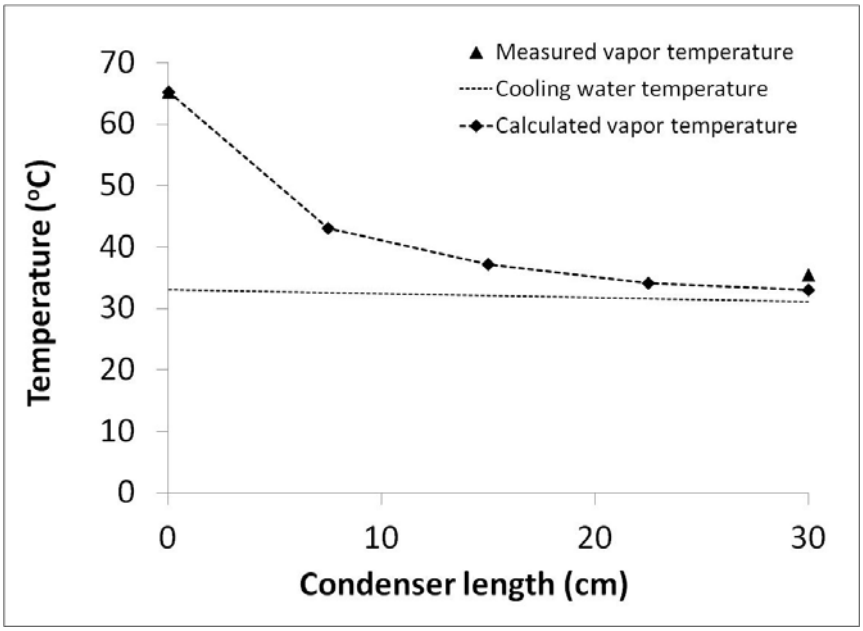

Figure 3: Temperature profile along the condenser ($T_{gas,\ inlet}$ = 65 °C, $T_{gas,outlet}$ = 36°C, $T_{cw,inlet}$ = 31 °C, $T_{cw,outlet}$ = 31°C).

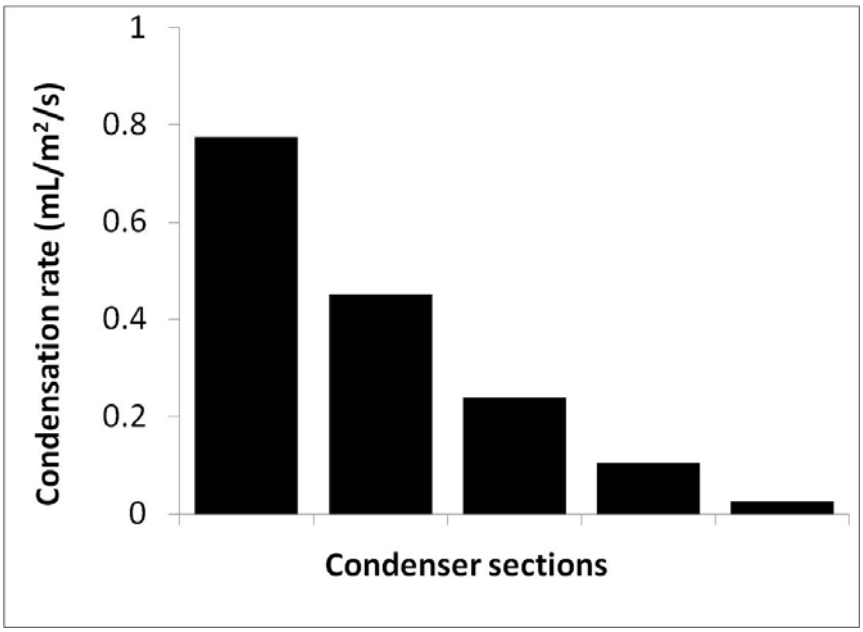

Figure 4: Water condensation rates corresponding to the temperature profile in Figure 3

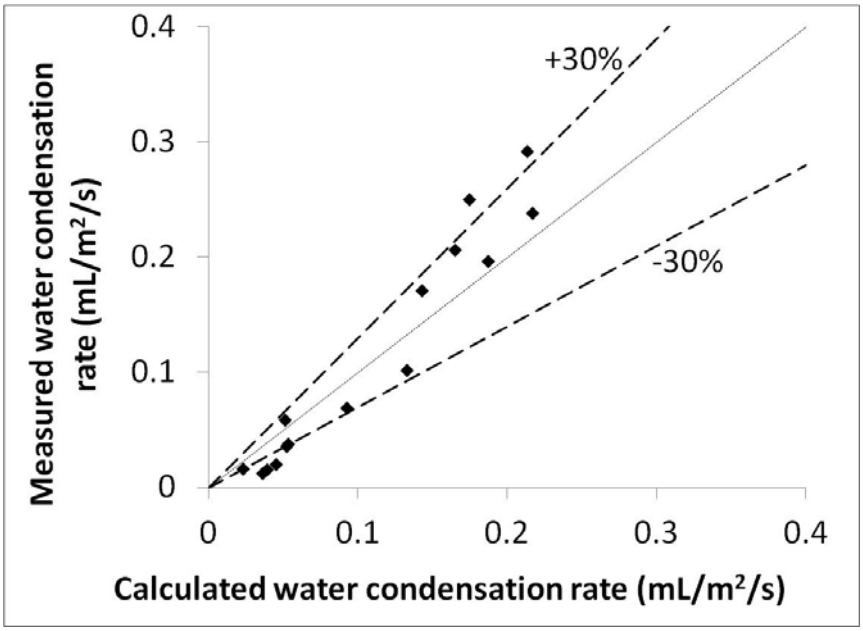

Figure 5: Comparison between calculated and measured water condensation rates.

Corrosion in pure water condensation

Figure 6 shows the corrosion rate as a function of water condensation rate for a variety of conditions. The samples located downstream in the condenser correspond to lower condensation rate conditions. Samples located upstream in the condenser were subjected to higher water condensation rates. In Figure 6, the corrosion rates obtained in stagnant condition, from a previous study, are also included.[4] Overall, the corrosion rate increases with water condensation rate, as was suggested to be the case by some previous studies. It should be pointed out that the CO_2 partial pressure (p_{CO2}) was not constant for all water condensation

rates. Increasing the temperature caused an increase in the partial pressure of water vapor and thus decreased p_{CO2}.

Figure 7 shows SEM images of the corroded samples corresponding to a condensation rate of 0.75 mL/m^2/s for 1 day and 3 day exposure time. The steel surface is partially covered with iron carbonate ($FeCO_3$) in the 1 day experiment and fully covered after the 3 day exposure. Even if the condensation rate was relatively high, $FeCO_3$ formed due to a higher steel surface temperature.

In a different scenario, a higher condensation rate condition corresponds to a lower cooling water temperature and therefore a lower steel surface temperature. In these conditions, no $FeCO_3$ formed (see Figure 8). This is because the kinetics of $FeCO_3$ formation is slower at lower temperature. In addition, saturation with respect to $FeCO_3$ plays an important role, as at high condensation rates, supersaturation is not easily achieved. On the other hand, for the downstream sample, the water condensation rate was very low. Thus, water droplets could stay in contact with the steel surface longer and the ferrous ion concentration within the droplets could build up sufficiently and lead to precipitation of $FeCO_3$.

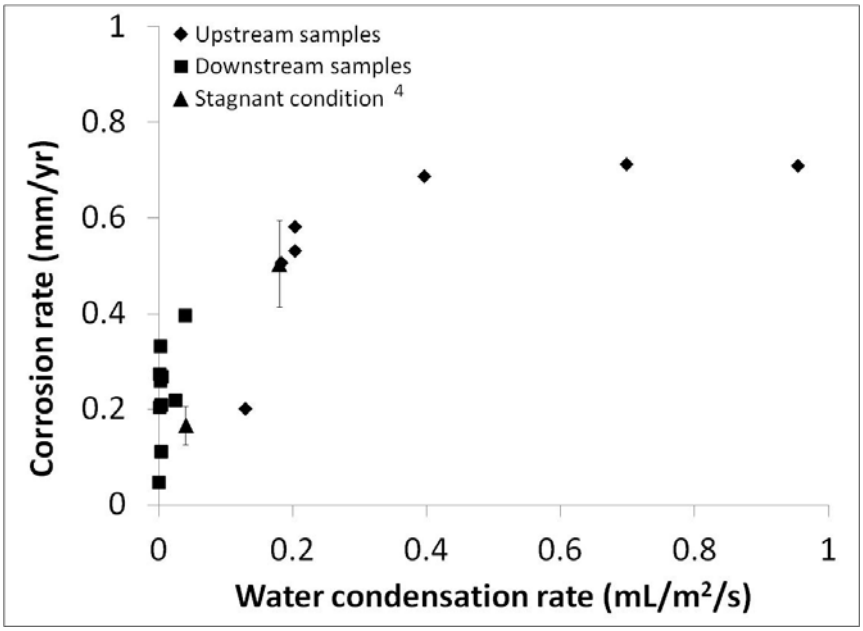

Figure 6: Corrosion rates at different condensation rates (T_{gas} = 18-65°C, Total P = 1 bar, p_{CO2} = 0.75-0.95 bar, test duration = 3 days)

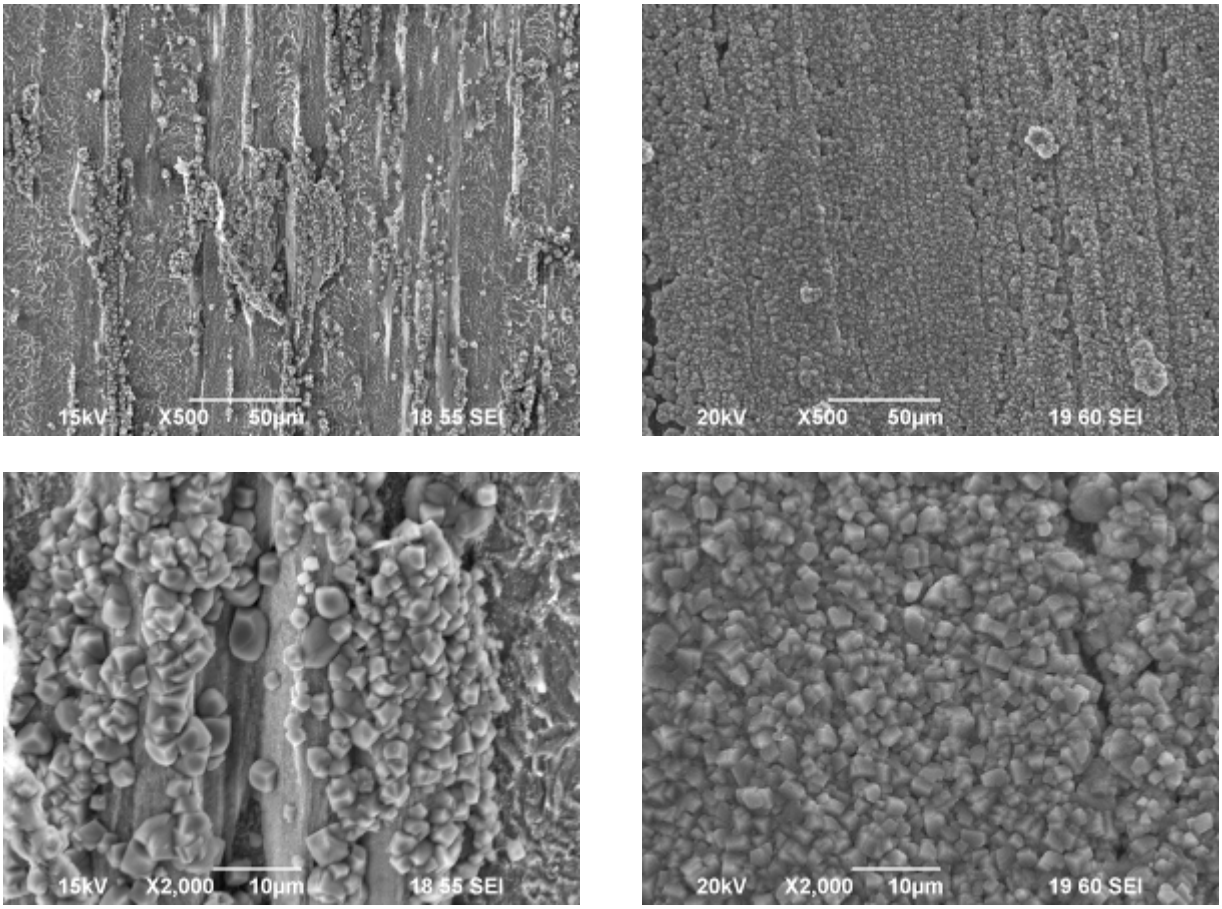

1 day 3 days

Figure 7: SEM Images of upstream samples exposed to condensation rate of 0.75 mL/m^2/s, T_{gas} = 65^{o}C, T_{cw} = 30^{o}C, at 1 day and 3 days.

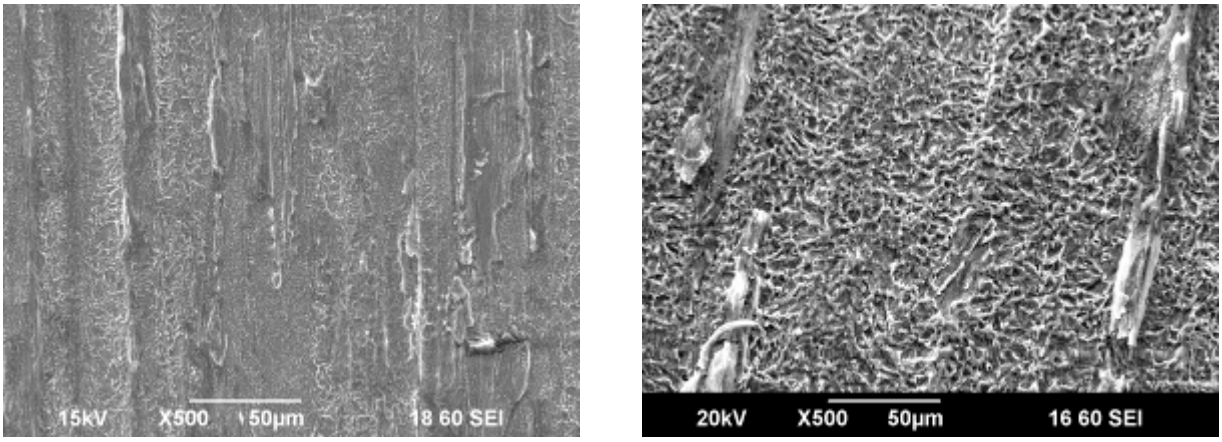

1 day 3 days

Figure 8: SEM Images of samples exposed to higher condensation rate of 1 mL/m^2/s, T_{gas} = 65^{o}C, T_{cw} = 16^{o}C, at 1 day and 3 days.

Corrosion in Co-condensation

Water and n-heptane are immiscible liquids and have similar vapor pressure at a given temperature. The “equilibrium ratio” condition refers to a fixed ratio of each component in the vapor phase, at a specific temperature. As shown in Figure 9, the equilibrium ratio of water to n-heptane vapor varies with vapor temperature.

A similar approach to that described above was used to determine the condensation rate for the upstream and downstream samples in the co-condensation experiments. Figure 10 shows a comparison of water and n-heptane integrated condensation rates from measurements and calculations. Good agreement was obtained.

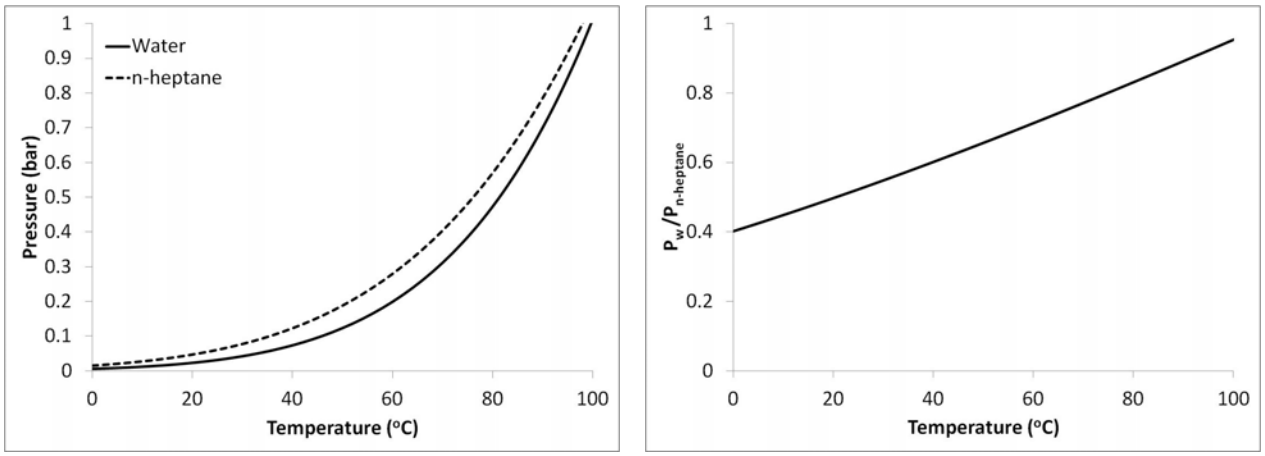

a b

Figure 9: a) Vapor pressure of water and n-heptane as a function of temperature and b) equilibrium ratio of the two components at various temperatures

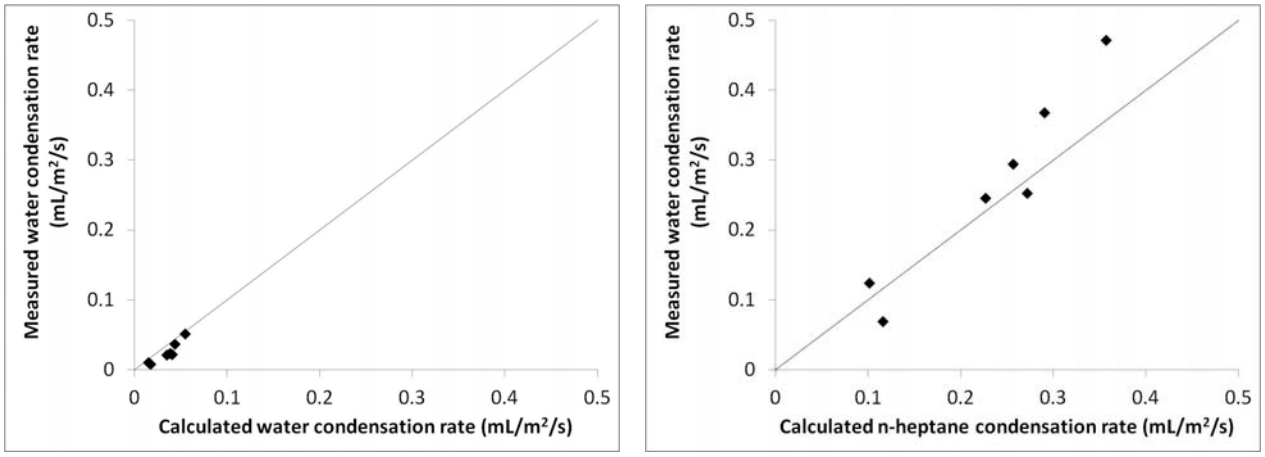

a b

Figure 10: Condensation rate comparison of a) water and b) n-heptane in the co-condensation scenario.

Figure 11 and Figure 12 show SEM images of carbon steel samples exposed to co-condensation, along with corresponding WCR and HCCR. The presence of n-heptane caused the disruption of the continuous water film and lead to segregation of distinct droplets of water

separated by n-heptane. The size of the water droplets condensing on the sample surface was related to the water condensation rate (Figure 11). When condensation rates of both liquids were relatively high, water droplets could be as large as 5 mm. Vice versa, with very low condensation rates, water droplets had a very small diameter of approximately 0.1 mm. In longer test duration (3 days) similar behavior was observed.

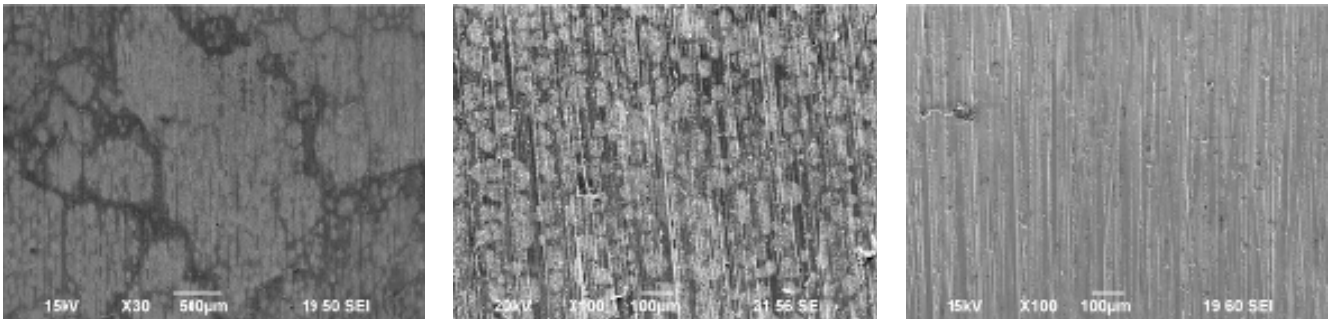

a.) T_{gas}/T_{cw} = 40/16.3°C
WCR = 0.14 mL/m^2/s
HCCR =0.91 mL/m^2/s

b.) T_{gas}/T_{cw} = 18/15.3 °C
WCR = 0.003 mL/m^2/s
HCCR = 0.021 mL/m^2/s

c.) T_{gas}/T_{cw} = 18/17.8 °C
WCR = 0.001 mL/m^2/s
HCCR = 0.007 mL/m^2/s

Figure 11 Surface morphology of carbon steel sample surface exposed to different co-condensation rates, HCCR is n-heptane condensation rate and WCR is water condensation rate (test duration = 1 day)

Figure 13 presents corrosion rates as a function of water condensation rate in a co-condensation scenario. Note that the condensation rate of n-heptane for the various conditions shown in this graph was not constant, rather it varied together with water condensation rate as shown on the secondary x-axis. In the 1 day-experiment, the corrosion rate increased with co-condensation rate, however not nearly as much as it did in pure water condensation experiments (see Figure 6). Extending the test duration to 3 days, not only showed a decline in corrosion rate with time, but also an even weaker dependency of corrosion rate on water condensation rate.

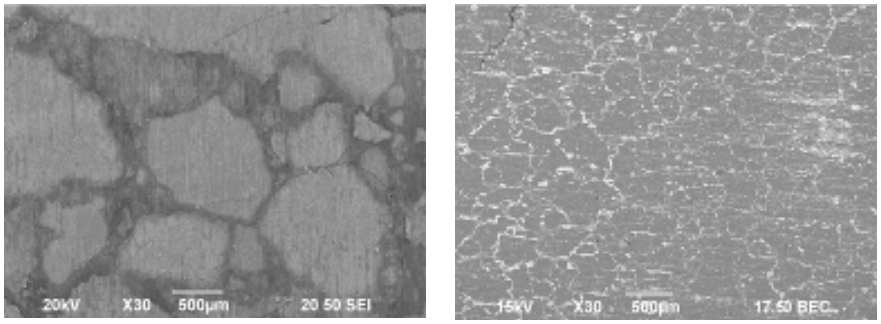

a.) T_{gas}/T_{cw} = 40/16.3°C
WCR = 0.16 mL/m^2/s
HCCR =1.1 mL/m^2/s

b.) T_{gas}/T_{cw} = 18/15.2
WCR = 0.001 mL/m^2/s
HCCR = 0.004 mL/m^2/s

Figure 12: Surface morphology of carbon steel samples exposed to different co-condensation rate, HCCR is n-heptane condensation rate and WCR is water condensation rate (test duration = 3 days)

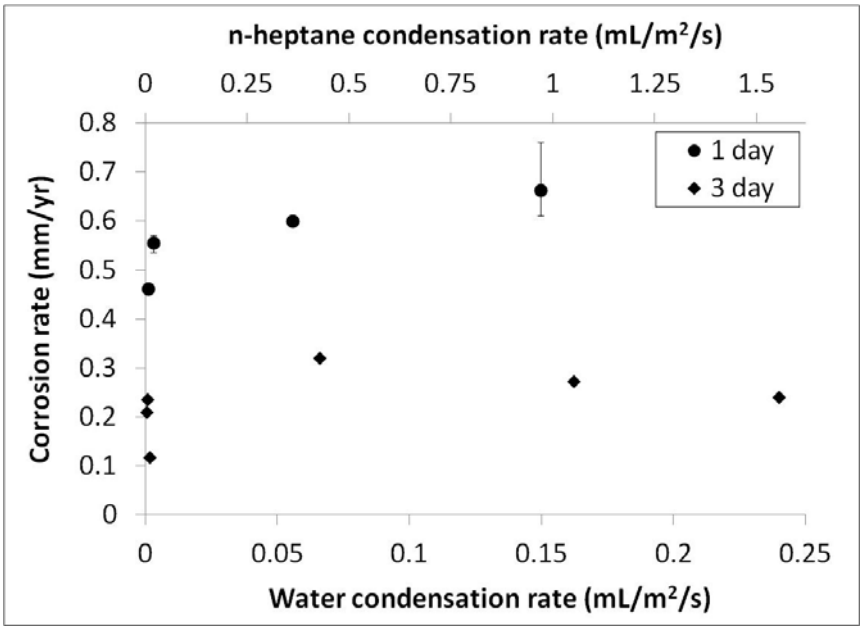

Figure 13: Corrosion rate in the co-condensation scenario as a function of condensation rate.

To illustrate this point, Figure 14 compares corrosion rates as a function of water condensation rate, in the absence and presence of n-heptane. In the absence of n-heptane, the corrosion rate increased with water condensation rate whereas no significant change was observed in the presence of n-heptane. The previous study of TLC under a stagnant vapor phase yielded similar behavior. Similar corrosion rates were measured in the low condensation rate range (WCR<0.1 mL/m^2/s) in the presence and absence of n-heptane. The difference was pronounced at much higher condensation rates.

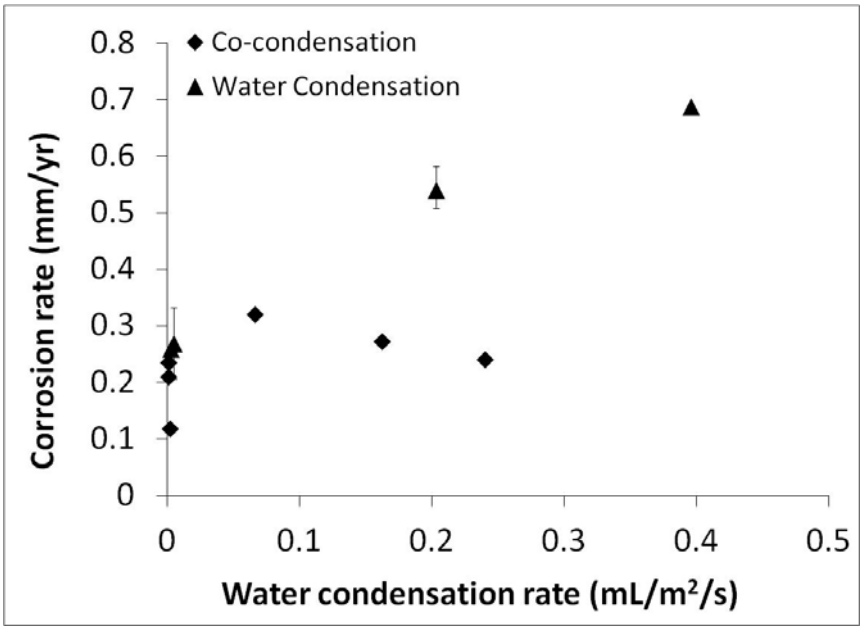

Figure 14: Corrosion rates in the absence and presence of n-heptane

There is a number of plausible explanations which can help us understand the influence of condensable hydrocarbons on TLC, as seen in Figure 14. They are listed below.

- *A decrease in partial pressure of CO_2*
  The present experimental setup limits the total pressure to 1 bar. The presence of n-heptane in the vapor phase partially replaces the CO_2. This decrease in partial pressure of CO_2 , which amounted to 20-30%, can lead to a small decrease in corrosion rate.

- *A decreased area of steel in contact with water*
  The amount of liquids co-condensed on the steel surface is overwhelmingly in favor of n-heptane: approximately 1 to 9 on a volume basis. Yet, the ratio of corroded to non-corroded area of the steel is almost inverse – strongly in favor of water (see Figures 11 and 12). This is because water has a stronger affinity for steel compared to n-heptane. Yet, uncorroded areas are present, indicating that hydrocarbons share a portion of the steel surface with water, shielding them form corrosion. Therefore, the corroded area in co-condensation experiments is not the full area of the samples, which was used in the corrosion rate calculations. This has resulted in somewhat lower uniform corrosion rates reported in Figure 13 and 14. However, the large discrepancy seen in Figure 14 cannot b explained by this factor alone.

- *Changes in condensed water chemistry*
  In all co-condensation experiment formation of $FeCO_3$ was observed. This strongly suggests a different water chemistry with higher concentrations of ferrous ion and higher pH, both leading to a lower corrosion rate.

While all the work presented above was done with n-heptane and water, it can be assumed that a similar corrosion behavior could be extrapolated to other condensable hydrocarbons, with some adjustments.

CONCLUSIONS

- The results show that TLC rate is less affected by the water condensation rate in the presence of co-condensation of n-heptane.
- It is thought that the water chemistry within condensed droplets was affected by co-condensation of n-heptane – the pH was higher and the formation $FeCO_3$ was facilitated – both leading to a lower corrosion rate.

ACKNOWLEDGEMENTS

The authors would like to acknowledge the technical guidance and financial support provided by the sponsor companies of the Top of the Line Corrosion Joint Industry Project at Ohio University: Total, BP, ConocoPhillips, Chevron, Saudi Aramco, Occidental Oil Company, ENI, and PTTEP.

REFERENCES

1. Y. Gunaltun, D. Supriyatman, and J. Achmad, “Top of line corrosion in multiphase gas lines. A case history,” CORROSION/99, paper no.99036 (Houston, TX: NACE, 1999).

2. M. Singer, S. Nesic, and Y. Gunaltun, “Top of the Line Corrosion in Presence of Acetic Acid and Carbon Dioxide,” CORROSION/04, paper no.04377 (Houston, TX: NACE, 2004).
3. D. V. Pugh, S.L. Asher, J. Cai, W.J. Sisak, J.L. Pacheco, F. Che Ibrahim, E.J. Wright, A. Dhokte, S. Venaik, and D. Robson, “Top-of-line corrosion mechanism for sour wet gas pipelines,” CORROSION/09, paper no. 09285 (Houston, TX: NACE, 2009).
4. T. Pojtanabuntoeng, M. Singer, and S. Nesic, “Water/Hydrocarbon Co-Condensation and the Influence on Top-of-the-Line Corrosion,” CORROSION/11, paper no. 11330, (Houston, TX: NACE, 2011).
5. W. Akers and M. Turner, “Condensation of vapors of immiscible liquids,” *AIChE Journal 8*, 5 (1962):p. 587–589.
6. S. H. Bernhardt, J. J. Sheriden, and J. W. Westwater, “Condensation of immiscible mixtures,” *AIChE Journal 68*, 118 (1972): p. 21-37.
7. A. Boyes and A. Ponter, “Condensation of Immiscible Binary Systems,” *CPE-Heat Transfer Survey*, (1972): p. 26-30.
8. X. Tang, C. Li, F. Ayello, J. Cai, S. Nesic, and C. T. Cruz, “Effect Of Oil Type On Phase Wetting Transition And Corrosion In Oil-Water Flow,” CORROSION/07, paper no. 07170, (Houston, TX: NACE, 2007).
9. F. Ayello, W. Robbins, and S. Richter, and S. Nesic "Crude oil chemistry effects on inhibition of corrosion and phase wetting," CORROSION/11, paper no. 11060, (Houston, TX: NACE, 2011).
10. J. Cai, C. De Waard, and S. Nesic, “Modeling of water wetting in oil-water pipe flow,” in CORROSION/04, paper no. 04663, (Houston, TX: NACE, 2004).
11. U. Lotz, L. van Bodegom, and C. Ouwehand, “The effect of type of oil or gas condensate on carbonic acid corrosion,” *Corrosion 47*, 8 (1991): p. 635-644.
12. ASTM G1, “Standard Practice for Preparing, Cleaning, and Evaluating Corrosion Test Specimens” (West Conshohocken, PA: ASTM).
13. F. Incropera, D. Dewitt, T. Bergman, A.Lavine, *Fundamental of Heat and Mass Transfer,* 6th ed. (Hoboken, NJ: John Wiley & Sons, 2006), p.497-504.